

Differential expression of Prominin-1 (CD133) and Prominin-2 in major cephalic exocrine glands of adult mice

József Jászai · Peggy Janich · Lilla M. Farkas ·
Christine A. Fargeas · Wieland B. Huttner ·
Denis Corbeil

Accepted: 22 August 2007 / Published online: 14 September 2007
© Springer-Verlag 2007

Abstract The major cephalic exocrine glands share many morphological and functional features and so can be simultaneously affected in certain autoimmune- and inherited disorders leading to glandular hypofunction. Phenotypic characterization of these exocrine glands is not only an interesting biological issue, but might also be of considerable clinical relevance. The major salivary and lacrimal glands might therefore be potential subjects of future cell-based regenerative/tissue engineering therapeutic approaches. In the present study, we described the expression of the stem and progenitor cell marker Prominin-1 and those of its paralogue, Prominin-2, in the three pairs of major salivary glands, i.e., submandibular-, major sublingual-, and parotid glands in adult mice. We have also documented their expression in the extraorbital lacrimal and meibomian glands (*Glandulae tarsales*) of the eyelid (*Palpebra*). Our analysis revealed that murine Prominin-1 and Prominin-2 were differentially expressed in these major cephalic exocrine organs. Expression of Prominin-1 was found to be associated with the duct system, while Prominin-2 expression was mostly, but not exclusively, found in the acinar compartment of these organs with marked differences among the various glands. Finally, we report that

Prominin-2, like Prominin-1, is released into the human saliva associated with small membrane particles holding the potential for future diagnostic applications.

Keywords Prominin · Salivary gland · Lacrimal gland · Meibomian gland · Membrane vesicles

Introduction

Accompanying the visual organ and the initial segment of the mammalian digestive system, the major exocrine glands of the head produce considerable amounts of watery secretion in forms of tear and saliva, respectively. These glands share significant structural and functional similarities, and their secretion is controlled by parasympathetic activity of the facial and glossopharyngeal nerves. The parenchyma of the major cephalic exocrine glands is composed of essentially two types of epithelial cells: acinar and ductal cells. The composition of the body fluids produced by the exocrine glands is well described. Except some degree of overlap/redundancy, each type of gland produces a special set of secreted products that is also reflected by the fine details of their histological structures (Denny et al. 1997). Besides inorganic ions, these body fluids contain variable amounts of proteinaceous and biologically active substances, e.g., enzymes, antibodies, and growth factors (Zelles et al. 1995; Gresik et al. 1996).

Reduced levels of salivary and/or lacrimal secretion results in xerostomia and xerophthalmia leading to consequent disease conditions, e.g., severe dental caries, oropharyngeal infections, ocular surface disorders. One of the most common causes of lacrimal and salivary gland hypofunction is the autoimmune exocrinopathy known as Sjögren's syndrome (van Blokland and Versnel 2002). In

J. Jászai · P. Janich · C. A. Fargeas · D. Corbeil (✉)
Tissue Engineering Laboratories, Biotec,
University of Technology Dresden,
Tatzberg 47-49, 01307 Dresden, Germany
e-mail: corbeil@biotec.tu-dresden.de

J. Jászai
e-mail: jozsef.jaszai@biotec.tu-dresden.de

L. M. Farkas · W. B. Huttner · D. Corbeil
Max-Planck-Institute of Molecular Cell Biology and Genetics,
Pfotenhauerstrasse 108, 01307 Dresden, Germany

the affected individuals dacryo- and sialoadenitis develops and finally the glandular parenchyma becomes atrophic. This disease frequently affects the meibomian gland of the eyelid as well (Shimazaki et al. 1998). The meibomian gland is a large sebaceous gland of the upper and lower eyelid that synthesizes and secretes lipids being important in preventing the evaporation of the tear film layered over the ocular surface, maintaining hence its integrity (McCulley and Shine 2004). The possibilities of pharmacological and/or gene therapy treatments in case of exocrine gland hypofunction are limited, especially if the quantity of the glandular secretory tissue is markedly reduced (Tran et al. 2005). The functional restoration of salivary/lacrimal secretion might, therefore, be better achieved by regenerative approaches based on (multipotent) tissue specific progenitor cell populations. Currently, many efforts are spent in identifying stem cells in adult organs that could provide a source for regenerative therapies aimed at functional restoration. The identification and isolation of such cell populations, however, require specific cell surface markers and detailed phenotypic characterization of the constituent cell populations of a given organ.

Interestingly, both the saliva and the tear are enriched in one of the most extensively studied somatic stem and progenitor cell marker, Prominin-1 (CD133) (Weigmann et al. 1997; Miraglia et al. 1997; Fargeas et al. 2003b, 2006). Prominin-1 is found to be associated in these body fluids with small membrane particles that are sedimented upon high-speed centrifugation (Marzesco et al. 2005; Dubreuil et al. 2007). The tissue compartments within the major cephalic exocrine glands, however, from which Prominin-1 might be derived are not yet documented. Prominin-1 is the founding member of an evolutionarily conserved family of integral pentaspan transmembrane glycoproteins (Fargeas et al. 2003a; for review see Corbeil et al. 2001a; Jászai et al. 2007). Mammalian species have a Prominin paralogue in their genomes, showing the typical pentaspan transmembrane topology characteristic of Prominin-1. This second, as yet, less characterized member of the protein family, shares only a moderate about 30% amino acid identity with Prominin-1 (Corbeil et al. 2001a; Zhang et al. 2002; Fargeas et al. 2003a). Mammalian Prominin-1 is expressed in several embryonic- and adult epithelia (Weigmann et al. 1997; Corbeil et al. 2000, 2001b; Lardon et al. 2007), epithelial-derived cells such as rod photoreceptor cells (Maw et al. 2000) and in non-epithelial cells, notably hematopoietic stem and progenitor cells (Yin et al. 1997; Corbeil et al. 2000). According to previous observations made on tissue dot blot arrays, expression of Prominin-2 exhibits a partial overlap with Prominin-1 in various embryonic and adult organs (Fargeas et al. 2003a; Florek et al. 2005). The subcellular localization of the two paralogues, however, is markedly distinct given that Prominin-2, in contrast to the

apically restricted expression of Prominin-1, is also displayed basolaterally (Florek et al. 2007; J. Jászai and D. Corbeil, unpublished data).

Here, we undertook by means of immunocytochemistry and in situ hybridization (ISH) analyses of the murine major salivary- and lacrimal-glands in order to reveal sites of Prominin-1 and Prominin-2 expression. We provide evidence for the expression of Prominin-2 in major cephalic exocrine glands and its release into the saliva. Detailed description of the expression of Prominin molecules has twofold importance. First, it might help the identification of potential tissue specific progenitor cell populations; second, monitoring changes in expression levels of Prominin molecules in excreted body fluids might be of diagnostic value in certain malignant tissue transformations and upon tissue replacement (Florek et al. 2005).

Materials and methods

Tissue samples

Mouse salivary and lacrimal gland samples were obtained from C57Bl6 strain. Young adult male mice (2–3 months) were deeply anesthetized by a single intra-peritoneal bolus injection of Ketamine and Xylazin mixture. Animals were then trans-cardially perfused with ice-cold 4% paraformaldehyde (PFA). The organs were removed and post-fixed in 4% PFA at 4°C for 2 h. After cryoprotection with 30% sucrose-PBS tissue samples were embedded in OCT compound (Tissue Tek, Sakura, The Netherlands). Samples were sectioned at 12 µm and then mounted onto SuperFrost Plus microscope slides (Menzel), dried overnight, and stored at –20°C until use.

Non-radioactive in situ hybridization

In situ hybridization on mouse sections was performed according to standard protocols (Tiveron et al. 1996). Briefly, serial sections were hybridized for 16 h at 70°C with digoxigenin (DIG) labeled cRNA probes (see below) at a concentration of 0.5 ng/µl. Stringency washes were performed at 70°C. The sections were then incubated with anti-DIG antibody (1:4000; Roche Molecular Biochemicals, Mannheim, Germany) for 16 h at 4°C. After several washing steps the reaction was visualized using NBT-BCIP substrate (Roche) giving a blue reaction product. After stopping the color reaction by several washes in PBS, the sections were rinsed quickly in dH₂O and then mounted with Kaiser's Glycerol-Gelatin (Merck, Darmstadt, Germany). Images were captured using an Olympus BX61 microscope with the IPLAB software.

Probes for in situ hybridization

Antisense complementary DIG-labeled ribonucleic acid (cRNA) probes were generated using T7 RNA polymerase (Roche) and DIG labeling mix (Roche). To synthesize murine Prominin-1 (Accession Number AF026269) and Prominin-2 (Accession Number AF269062) cRNA probes a 2.1 kb (nt 198–2,264) and a 1.9 kb (nt 346–2,258) cDNA fragment was used, respectively.

Immunohistochemistry

Immunofluorescent detection of Prominin-1 on serial cryostat sections was performed as follows. Cryosections were brought to room temperature and washed twice with PBS. Sections were incubated with 0.005% SDS in 0.2% gelatin-PBS for 30 min. The samples were then rinsed with 0.2% gelatin-PBS followed by three changes of 0.15% saponin in 0.2% gelatin-PBS for 30 min each. Sections were incubated overnight with anti-Prominin-1 antibody, i.e., rat monoclonal antibody (mAb) 13A4 (1:400; Weigmann et al. 1997) in 0.15% saponin in 0.2% gelatin-PBS at 4°C. The samples were then extensively washed with 0.15% saponin in PBS followed by a washing step with 0.15% saponin in 0.2% gelatin-PBS for 30 min. The primary antibody was detected using a goat anti-rat Cy3-conjugated secondary antibody (1:1,000; Jackson Lab, Bar Harbor, ME, USA) in 0.15% saponin in 0.2% gelatin-PBS. The samples were then extensively washed in 0.15% saponin in PBS and rinsed once with PBS. In order to facilitate the identification of the tubular segments of the exocrine glands according to their typical nuclear configurations the slides were counterstained with DAPI. After washing once with PBS, the slides were mounted with Mowiol. Images were captured using an Olympus BX61 compound microscope with the IPLAB software. The composite images were prepared from the digital data files using Adobe Photoshop and Illustrator.

Saliva and differential centrifugation

Saliva was obtained from healthy volunteers with informed consent and prepared as previously described (Marzesco et al. 2005). Samples were subjected to differential centrifugation steps (all done at 4°C): 5 min at 300g, supernatant 10 min at 1,200g, supernatant 30 min at 10,000g, supernatant 1 h at 200,000g, and supernatant 1 h at 400,000g. The resulting pellets were resuspended in 40 µl SDS sample buffer and an equal volume (10 µl) for each protein samples have been loaded on a SDS-PAGE gel followed by immunoblotting for either prominin-1 or prominin-2 (see below).

Endoglycosydase digestion and immunoblotting

The 200,000g pellet of saliva obtained after differential centrifugation and as positive control, CHO cells transfected with human Prominin-2 cDNA plasmid (Fargeas et al. 2003a), were incubated in the absence or presence of 1 U peptide-N-glycosidase F (PNGase F) according to the manufacturer's instructions (Roche). The protein samples were subjected to SDS-PAGE (7.5%) followed by immunoblotting as previously described (Marzesco et al. 2005) using either mouse mAb anti-human Prominin-2 (mAb 2024, clone 244029; 1:000; R&D Systems, Minneapolis, MN, USA) or our novel mouse mAb α hE2 (1 µg/ml; Missol-Kolka et al. manuscript in preparation) directed against a fragment of the first extracellular loop of human Prominin-1; see also Florek et al. 2005). In both cases, the antigen-antibody complexes were revealed using horseradish-peroxidase-conjugated secondary antibodies followed by enhanced chemiluminescence (ECL System, Amersham, Piscataway, NJ, USA).

Anatomical terminology

To designate a particular anatomical structure, we have simultaneously used the English terminology gaining increasing popularity and the traditional Latin anatomical terminology based on *Nomina Anatomica Veterinaria* (NAV) and *Terminologia Anatomica* (TA).

Results

Previous dot blot analysis of both *Prominin-1* and *Prominin-2* transcripts suggested that they might be expressed by salivary glands (Fargeas et al. 2003a; Florek et al. 2005), but no information was available about their expression and tissue compartmentalization in these exocrine glands. We therefore decided to analyze their distribution in adult murine salivary- and lacrimal-glands by means of immunocytochemistry and ISH. Since we have previously identified murine Prominin-1 in a mAb screening (Weigmann et al. 1997), we have applied the same well-characterized mAb 13A4 throughout the present study, while the expression of Prominin-2 was revealed by ISH given that currently no specific antibody is available against the murine protein for immunocytochemical detection (Fargeas et al. 2003a).

Expression of Prominin-1 and Prominin-2 in the major salivary glands

Submandibular gland (Glandula submandibularis)

Among the salivary glands in rodents, the submandibular gland seems to be the largest and most complex one. The

parenchyma of the gland consists of seromucous secretory acini and a particularly well-elaborated duct system. The duct system is composed of intercalated ducts, granular convoluted tubules (especially in males), intra-lobular striated ducts, interlobular excretory ducts and a main excretory duct (Tandler 1993). Immunofluorescent staining of Prominin-1 revealed an intense labeling of the intercalated ducts (Fig. 1a, red, white arrowheads) that are easily identified based on their characteristic morphology on DAPI counterstained specimen (Fig. 1a, blue). In these ducts Prominin-1 immunoreactivity was strictly confined to the apical domain of the epithelial cells (Fig. 1a'), as previously demonstrated for other epithelia (Weigmann et al. 1997; Corbeil et al. 2000). Other parts of the parenchyma including the seromucous acini (Fig. 1a, dashed lines) and the striated ducts (Fig. 1a, white hollow arrows) were negative. The distribution pattern of expression sites of *Prominin-2* transcripts was scattered "salt and pepper"-like corresponding to seromucous acini (Fig. 1b, b', black asterisks, blue). The duct system, however, appeared to be negative for *Prominin-2* including the well-developed granular convoluted tubules (Fig. 1b, b', white hollow arrows). The corresponding sense probe did not reveal any labeling (data not shown).

Parotid gland (*glandula parotis*)

The rodent parotid gland in contrast to its human counterpart is not the largest of the salivary glands. In spite of that the major secretory elements of the rodent parotid gland, just like in human, are the serous exocrine acini. The serous secretory elements are connected to a well-developed duct system composed of intercalated ducts (*tubulus intercalaris*), striated (*tubulus salivialis*), and excretory ducts. Immunofluorescence of Prominin-1 revealed an intense apical labeling of the intercalated ducts (Fig. 2a, b, white arrowheads) very reminiscent of the staining observed in the submandibular gland whereas the larger bore ducts (Fig. 2a, b, white hollow arrows) and the rest of the parenchyma containing serous acini appeared to be negative (Fig. 2a, b, dashed lines). *Prominin-2* was detected by non-radioactive ISH in serous acini (Fig. 2c, d, black asterisks) and, in contrast to what appeared in the submandibular gland, in all segments of the duct system including the striated and excretory ducts (Fig. 2c, d, black hollow arrows).

Major sublingual gland (*glandula sublingualis major*)

Topographically, the major sublingual gland appears to be very tightly associated with the submandibular gland separated only by a sheet of connective tissue (Hebel and Stromberg 1976). Nevertheless, microscopically its parenchyma appears to be significantly different from those of the submandibular gland. In rodents, just like in the human

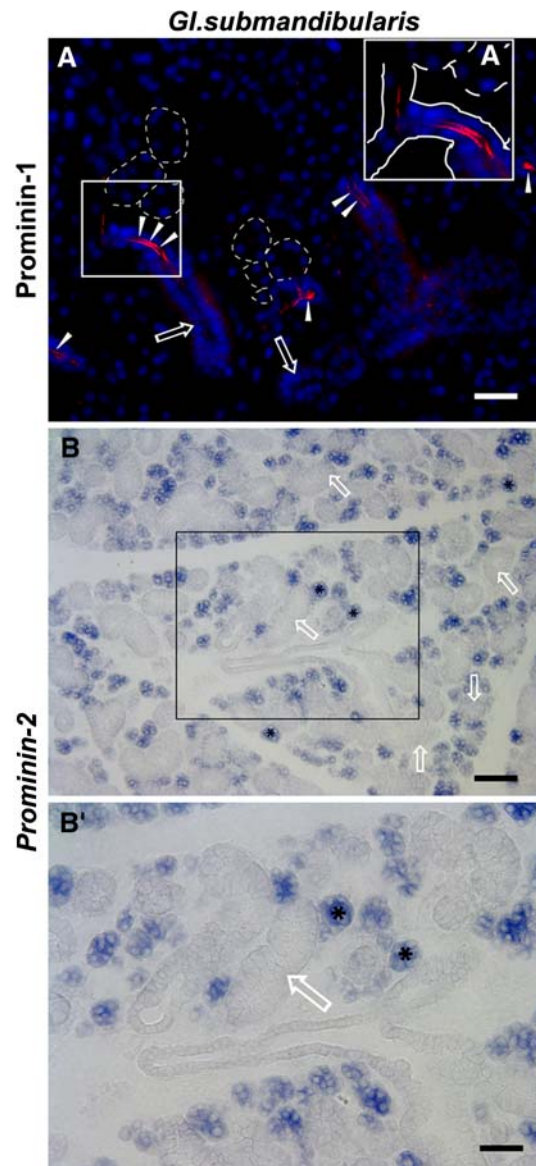


Fig. 1 Localization of Prominin-1 and *Prominin-2* in murine submandibular gland. Cryosections of submandibular gland were processed either for immunohistochemistry (**a**, **a'**, Prominin-1) or for non-radioactive in situ hybridization (**b**, **b'**, *Prominin-2*). **a**, **a'** Sections were immunolabeled with mAb 13A4 followed by Cy3-conjugated secondary antibody (red). To visualize nuclear architecture of the various structures within the glands, sections were counterstained with DAPI (blue). Intercalated ducts display a Prominin-1 staining (white arrowheads), while other parts of the parenchyma of the submandibular gland are negative. Some secretory acini are outlined by white dashed line and hollow white arrows indicate the striated ducts. Note that Prominin-1 immunoreactivity is confined to the apical surface of the epithelial cells (**a'**, white lines indicate the basal cell domain). **b**, **b'** Sections were hybridized with antisense DIG-labeled Prominin-2 probe. The seromucous acini of the submandibular gland are strongly positive (blue) for *Prominin-2* transcripts appearing in a scattered fashion (black asterisks). Other parts of the parenchyma are negative. Hollow white arrows point the granular convoluted tubules of the parenchyma. The inset in panel B demarcates a region displayed at higher magnification in **b'**. *Gl* Glandula according to NAV and TA. Bars 25 μ m in **a**; 100 μ m in **b**; 50 μ m in **b'**

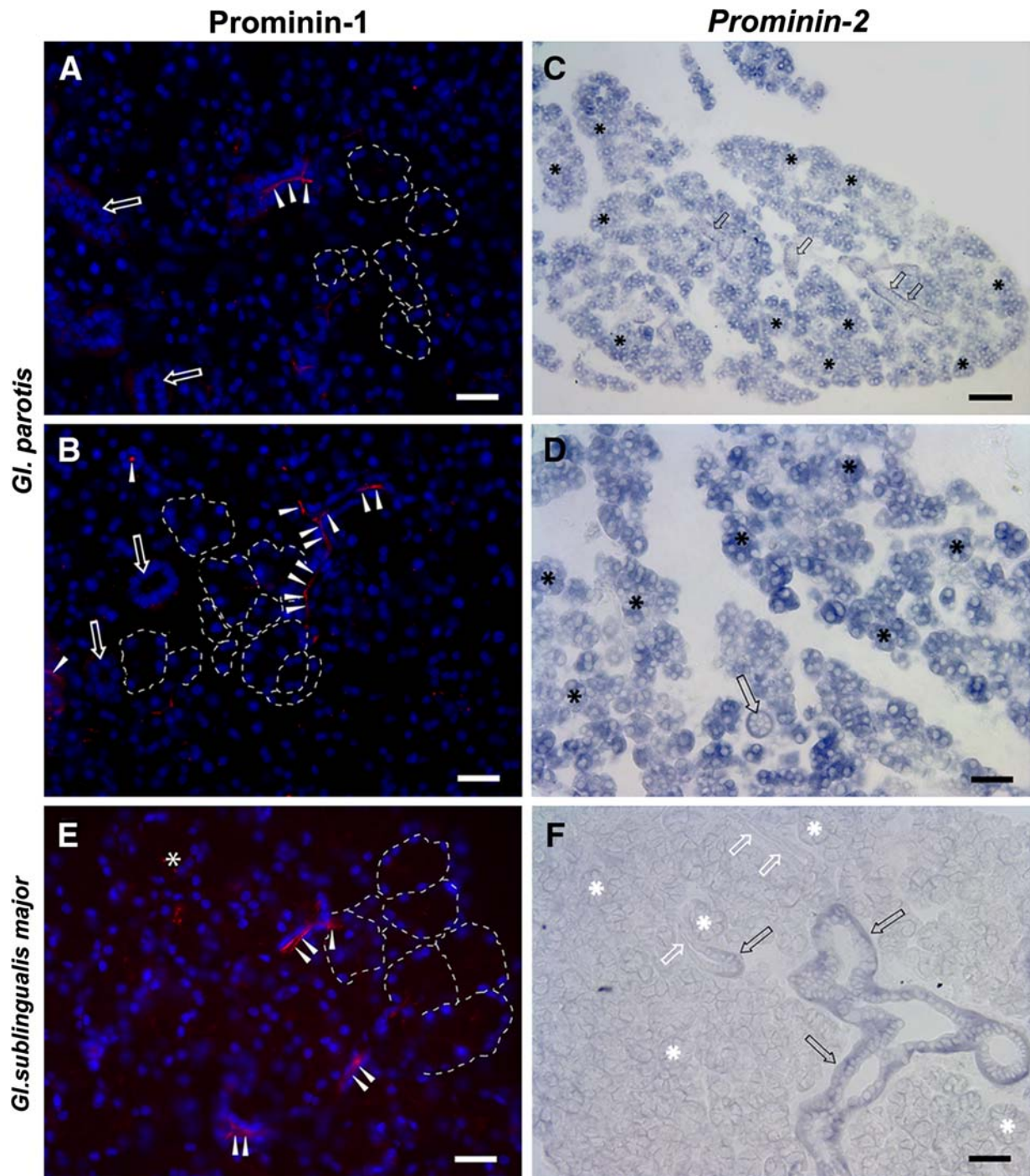


Fig. 2 Localization of Prominin-1 and *Prominin-2* in murine parotid and sublingual glands. Cryosections of parotid and sublingual glands were processed either for immunohistochemistry (**a, b, e**, Prominin-1) or for non-radioactive in situ hybridization (**c, d, f**, *Prominin-2*). **a, b, e** Sections were immunolabeled with mAb 13A4 followed by Cy3-conjugated secondary antibody (red). To visualize nuclear architecture of the various structures within the glands, sections were counterstained with DAPI (blue). **a, b** The intercalated ducts of the parotid gland display a Prominin-1 staining (white arrowheads). Hollow white arrows and white dashed lines indicate the absence of immunoreactivity in larger bore striated ducts and secretory acini, respectively. **e** The intercalated ducts of the major sublingual gland are highlighted by an

intense Prominin-1 staining (white arrowheads). Some secretory acini are outlined by white dashed line. White asterisk indicates the background observed when the primary antibody is omitted. **c, d, f** Sections were hybridized with antisense DIG-labeled Prominin-2 probe. **c, d** The parotid gland shows a robust expression of *Prominin-2* transcripts. Both the serous acini (black asterisks) and the duct system (hollow black arrow) are labeled. **f** Larger bore salivary ducts of the major sublingual gland are positive for *Prominin-2* transcripts (hollow black arrow). The negative mucous end-pieces and the intercalated ducts are indicated with white asterisks and hollow white arrows, respectively. *Gl* Glandula according to NAV and TA. Bars 25 μ m in **a, b, e**; 50 μ m in **d, f**; 100 μ m in **c**

being, the major sublingual gland is composed of mucous secretory endpieces (acini) or tubules capped with serous (Gianuzzi's or Ebner's) demilunes (Denny et al. 1997). The excretory duct system seems to be less complex than in the submandibular gland. Immunofluorescence of Prominin-1 revealed its expression in the intercalated ducts (Fig. 2e, white arrowheads) similar to the submandibular and parotid gland (see above). The rest of the parenchyma containing higher order parts of the duct system and the acini seemed to lack Prominin-1 expression (Fig. 2e). As for *Prominin-2*, significant differences in comparison to the other two major salivary glands were observed. The major sublingual gland showed a restricted distribution of *Prominin-2* transcripts. While the larger bore excretory ducts were positive for *Prominin-2* (Fig. 2f, black hollow arrows), the intercalated ducts were devoid of its transcript (Fig. 2f, white hollow arrows). The mucous end-pieces were also negative for *Prominin-2* transcripts (Fig. 2f, white asterisks) as opposed to the serous acini of the parotid or the seromucous acini of the submandibular gland.

Expression of Prominin-1 and Prominin-2 in the extraorbital lacrimal gland

The histological structure of the extraorbital lacrimal gland is very reminiscent of the serous parotid gland, however, its duct system is less elaborated. The secretory end-pieces are of serous character. Immunofluorescent detection of Prominin-1 showed an intense apical staining of both the intercalated tubules (Fig. 3a, b, white arrowheads) and larger bore intra-lobular ducts (Fig. 3b, white arrows; see also 3b'), while the serous end-pieces were immunonegative (Fig. 3a, dashed lines). Expression of *Prominin-2* in the serous acini of the extraorbital lacrimal gland, just like in those of the parotid gland or the seromucous end-pieces of the submandibular gland, was rather intense (Fig. 3c, black asterisks), while the duct system was negative (Fig. 3c, white hollow arrows).

Expression of Prominin-2, but not Prominin-1, in the eyelid

The mammalian eyelid is a complex anatomical structure. It contains diverse secretory elements being the meibomian gland (*Glandulae tarsales*) the largest and most complex one among those. The adult meibomian glands of the *tarsus* are lipid secreting holocrine sebaceous glands. Non-radioactive ISH with specific antisense DIG-labeled cRNA probes on adult eyelid specimen revealed a spatially restricted expression for *Prominin-2* and the absence of *Prominin-1* (Fig. 4). *Prominin-2* transcripts were strongly expressed in the acini of the meibomian gland (Fig. 4a, a', b, black arrows, a), and the root-sheath (Fig. 4a, a', black arrowheads) of the eyelash/*Cilium* (Fig. 4a, a', black hollow arrow; b, circle, c). In contrast, these structures expressed

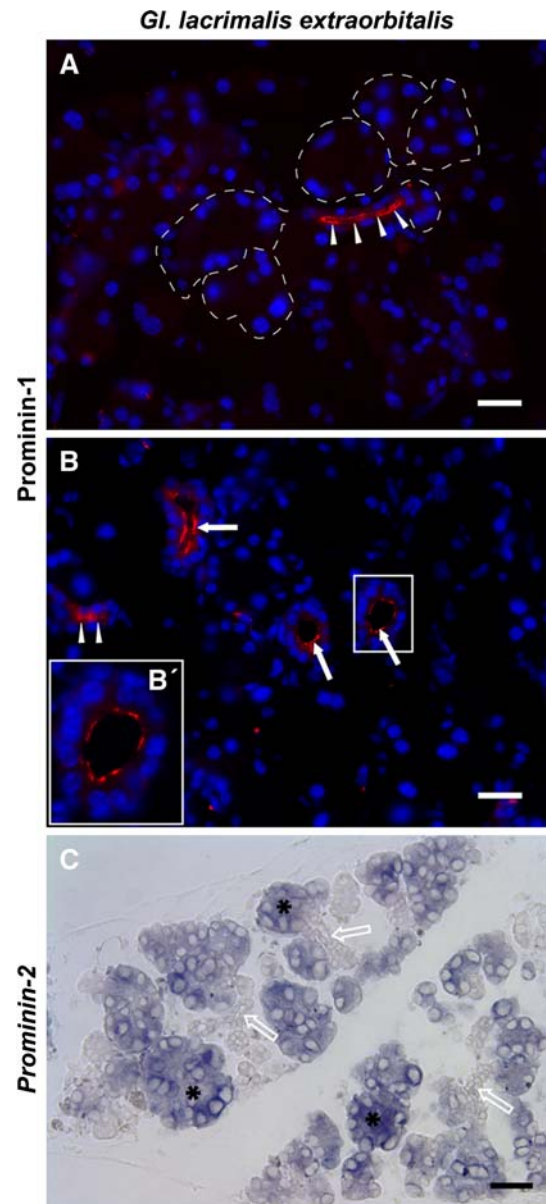


Fig. 3 Localization of Prominin-1 and *Prominin-2* in murine extraorbital lacrimal gland. Cryosections of extraorbital lacrimal gland were processed either for immunohistochemistry (a, b, b', Prominin-1) or for non-radioactive in situ hybridization (c, *Prominin-2*). a, b, b' Sections were immunolabeled with mAb 13A4 followed by Cy3-conjugated secondary antibody (red). To visualize nuclear architecture of the various structures within the glands, sections were counterstained with DAPI (blue). The intercalated ducts (white arrowheads) and larger bore lacrimal gland ducts (white arrows) of the extraorbital lacrimal gland are labeled. Some serous end-pieces are outlined by white dashed line. Note that Prominin-1 immunoreactivity is confined to the apical surface of the epithelial cells (b'). c Sections were hybridized with antisense DIG-labeled *Prominin-2* probe. The serous acini are positive for *Prominin-2* transcripts (black asterisks). White arrows point the negative intercalated ducts. *Gl* Glandula according to NAV and TA. Bars 25 μ m in a, b; 50 μ m in c

neither *Prominin-1* mRNA (Fig. 4c) nor its protein product as revealed by immunohistochemistry (data not shown). Besides the standard sense controls (data not shown), the

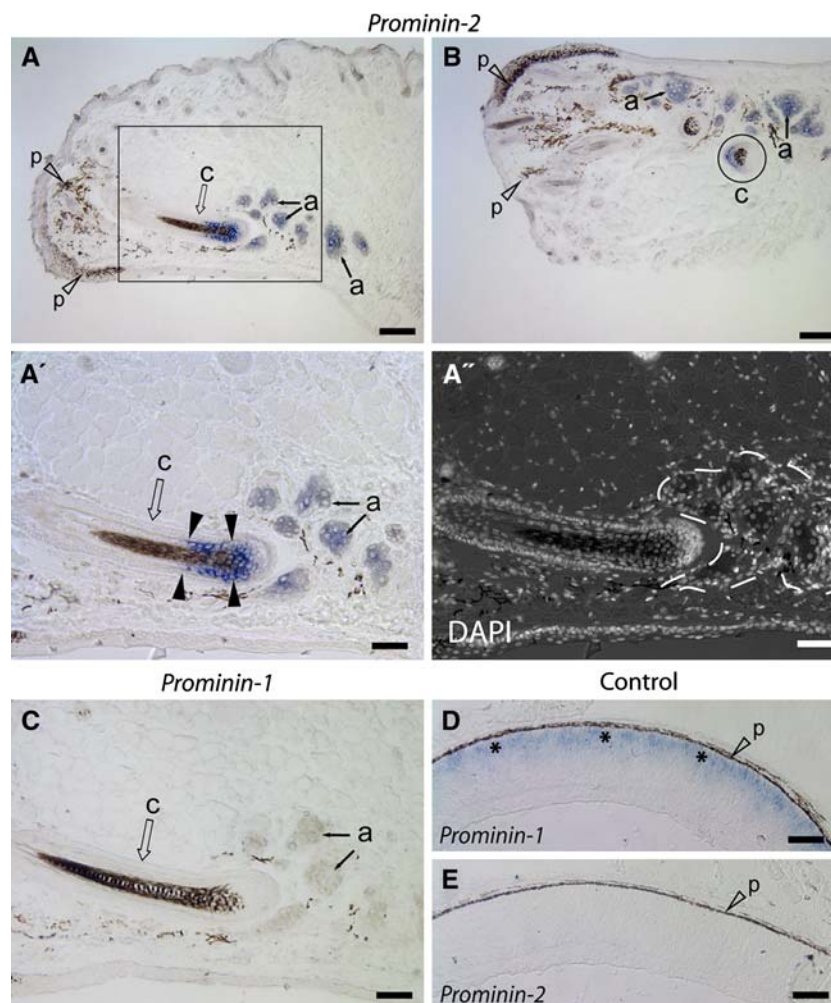


Fig. 4 Localization of *Prominin-2* transcripts in the murine eyelid (*Palpebra*) by non-radioactive in situ hybridization. Cryosections of the eyelid (**a**, **a'**, **b**, **c**) and retina (**d**, **e**) were hybridized with an anti-sense DIG-labeled probe specific for either *Prominin-2* (**a**, **a'**, **b**, **e**) or *Prominin-1* (**c**, **d**). The eyelid shows an intense *Prominin-2* labeling (**blue**) in the acini (**a**) of the meibomian gland (**black arrows**). The inset in panel **A** demarcates a region displayed at higher magnification in **a'** and a bright field view with a DAPI counterstained nuclei (**white**) is presented in **a''** where the region of the tarsal gland is surrounded by **white dashed line**. An eyelash/cilium (**c**), hit longitudinally by sectioning **a**, **a'** (**black hollow arrow**), shows a strong *Prominin-2* labeling in

the cells located in its root (**black arrowheads**). Slanted cross-section profile of a labeled eyelash root (**encircled**) is presented in panel **B**. The **brown color** observable in a scattered fashion is due to the natural pigmentation (**p**, **white hollow arrowheads**). **c** Both the acini (**a**), and eyelash/cilium (**c**) are negative for *Prominin-1* transcripts. **d**, **e** As ISH controls, the presence of *Prominin-1* transcripts in the outer nuclear layer of the retina derived from a postnatal-day-one mouse is documented (**d**, positive control, **black asterisks**) whereas *Prominin-2* transcripts are absent (**e**, negative control). The pigmented epithelium (**p**) is indicated with a **white hollow arrowhead**. Bars 100 μm in (**a**, **b**, **d**, **e**); 50 μm in (**a'**, **a''**, **c**)

specificity of the DIG-labeled antisense *Prominin-1* and *Prominin-2* probes was verified by simultaneous processing of murine eye samples (Fig. 4d, e), known to be enriched for *Prominin-1* transcripts (Fig. 4d, black asterisks) while lacking *Prominin-2* expression (Fig. 4e).

Detection of both Prominin molecules in the human saliva

The primary saliva secreted by acinar cells is not only conducted but its contents are also modified by the duct system (Tandler 1993). A plethora of biologically active substances, e.g., NGF, EGF, TGF- α , and HGF, are secreted

into the saliva especially by the striated ducts and granular convoluted cells (Gresik et al. 1996; Kagami et al. 2000; Tandler et al. 2001). The presence of membrane-tethered molecules in excreted body fluids, however, is scarcely documented. We have previously shown that Prominin-1 is associated with small membrane particles that are released into several human body fluids including the saliva and urine (Marzesco et al. 2005). Prominin-2 was also detected in the urine (Florek et al. 2007). Therefore, we investigated whether Prominin-2 could be released as well into the saliva by immunoblotting using a novel mAb 2024 directed against human Prominin-2. Interestingly, we observed in

saliva from healthy human donors a 112 kDa-immunoreactive band (Fig. 5a, lane 3, arrowhead), which is the expected molecular mass of Prominin-2 (Fargeas et al. 2003a). The authenticity of the 112 kDa-immunoreactive band was further verified by comparison with human Prominin-2 expressed transiently in CHO cells (Fig. 5a, lane 1). No immunoreactivity was detected when CHO cells were transfected with the empty expression vector (data not shown). An additional immunoreactive band was detected in saliva (Fig. 5a, lane 3, asterisk). The identity of this protein is unknown but it appears to be insensitive to the N-deglycosylation by PNGase F (Fig. 5a, lane 4, asterisk) in contrast to Prominin-2 (Fig. 5a, lanes 2, 4, arrowhead). The loss of the Prominin-2 immunoreactivity upon PNGase F treatment (Fig. 5a, lanes 2, 4) suggests that the 2024 epitope of human Prominin-2 is partly dependent on N-glycosylation, and hence might be sensitive to conformational alteration.

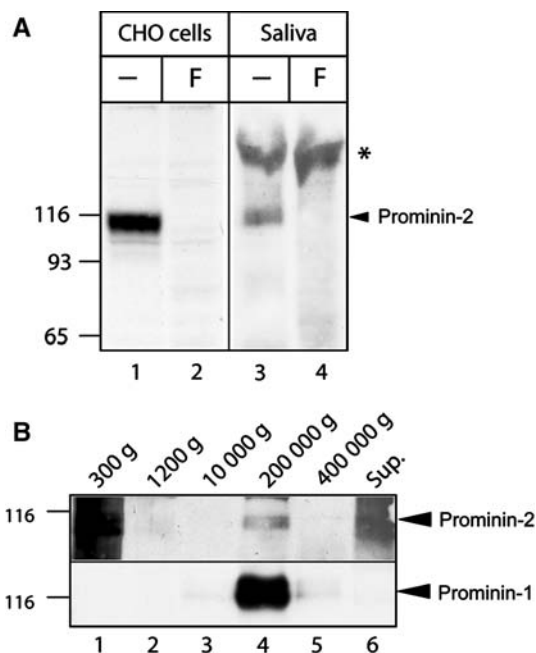


Fig. 5 Prominin-2-containing membrane particles are found in human saliva. **a** Proteins from saliva samples, and for comparison those from an extract of CHO cells transiently transfected with human Prominin-2 plasmid, were incubated in the absence (*dash*) or presence (*F*) of PNGase F and analyzed by immunoblotting with mouse mAb 2024. Note that upon deglycosylation the Prominin-2 immunoreactivity is lost in both saliva and Prominin-2-transfected CHO cell samples. *Arrowhead*, Prominin-2; *asterisk*, PNGase F-insensitive immunoreactive band of unknown identity. **b** Saliva samples were subjected to differential centrifugation and the resulting pellets analyzed by immunoblotting for the presence of either Prominin-2 or Prominin-1 using mAb 2024 and mAb zhE2, respectively. Saliva samples were centrifuged for 5 min at 300g, 10 min at 1,200g, 30 min at 10,000g, 1 h at 200,000g, and 1 h at 400,000g. Proteins in the 400,000g supernatant (*Sup*) were analyzed in parallel. *Arrowheads* indicate the corresponding prominin immunoreactive band. The position of prestained apparent molecular mass markers (in kDa) is indicated on the *left*

Upon differential centrifugation of saliva followed by immunoblotting of the resulting fractions Prominin-2 was detected in the 200,000g pellet (Fig. 5b, top panel, lane 4). Prominin-1 is also detected there (Fig. 5b, bottom panel, lane 4) in accordance with previous results (Marzesco et al. 2005). However, the expression level of Prominin-2 was modest in comparison with that of Prominin-1, which might reflect either a lower affinity of the anti-prominin-2 antibody—because of the putative conformational dependence of its epitope as suggested by the PNGase F treatment (see above)—or a distinct subcellular compartmentalization of both molecules (see Discussion). Taken together, our data indicate that saliva contains Prominin-2-containing membrane particles that are sedimented upon high-speed centrifugation.

Discussion

We described here the expression of Prominin-1 and its paralogue, Prominin-2, in the three major salivary glands, the lacrimal glands as well as in the palpebral meibomian gland. The major finding was the demonstration of their differential expression in these parenchymal organs. Prominin-1 was preferentially located in one particular segment of the duct system, while Prominin-2, depending on the particular gland, was found either in acinar cells or duct cells or in both compartments. The expression of Prominin-1 by intercalated duct cells of the major cephalic exocrine glands exemplifies the essential similarities existing between these ectodermal organs. However, the findings concerning expression of Prominin-2 point toward the fundamental differences detectable in the fine details of histology and microscopic anatomy of the serous and mucous exocrine glands.

The functional co-operation and topographical proximity of the major salivary glands are also reflected by similarities in the initiation of the developmental programs (Denny et al. 1997). All three pairs of major salivary glands are subject to a similar morphogenetic program involving reciprocal inductive interactions between the oral epithelium and the condensing neural crest-derived mesenchyme (Cutler and Gremski 1991; Denny et al. 1997). Furthermore, salivary gland phenotypes associated with mutations in the FGF signaling pathway reveal a crucial role of this signaling cassette both in salivary and lacrimal gland development (Entesarian et al. 2005). Detection of Prominin-1 in the intercalated ducts of the adult exocrine glands, i.e., salivary and lacrimal glands, is consistent with the significant similarities that these glands might share beyond the developmental period. Besides the comparable patterns of branching morphogenesis, however, there are striking differences among the individual organs. These differences

are reflected not only by substantial differences in the timing of functional differentiation but also by the distinct cellular composition/basic histological structures of each gland (Hand et al. 1996; Denny et al. 1997; Patel et al. 2006). For instance, development of both the submandibular and parotid glands includes a prolonged postnatal period of cytodifferentiation (Cutler and Chaudhry 1974, 1975), whereas this process is complete at birth in the sublingual gland (Redman and Ball 1978; Wolff et al. 2002). Accordingly, acinar secretory cells of the different adult glands display distinct, only partially overlapping, biochemical phenotypes (Hand et al. 1996). The differential expression of Prominin-2 further underlines this notion at least in the relation of serous/seromucous versus mucous acini, as Prominin-2 was not detectable in the latter ones of the major sublingual gland.

Among the three pairs of major salivary glands in rodents, the submandibular gland represents the most complex system. It is a dynamically changing parenchymal organ with marked signs of sexual dimorphism in mice (Gresik and MacRae 1975; Gresik 1994). Its histodifferentiation is delayed, achieving completion only at puberty. The permanent re-structuring of the submandibular gland parenchyma due to the elaboration of the duct system is under the control of intricate developmental, hormonal (androgen), and neural regulatory network (Gresik 1994; reviewed in Denny et al. 1997). However, how the fate decisions are made in such a complex system is far from being understood. With maturation of the salivary glands, multiple cell types emerge as a result of transformation/trans-fating. Nevertheless, some of the intercalated duct cells seem to retain features characteristic of a perinatal, less differentiated state at least in the adult submandibular gland (Man et al. 1995). The retention of this phenotype resembling of type I/terminal tubule perinatal acinar cells suggests that these cells might act as progenitors for other parenchymal cell types explaining the regenerative capacity (Takahashi et al. 1998; Okumura et al. 2003) and homeostatic cell replacement (Zajicek et al. 1985; reviewed in Denny et al. 1997; Denny and Denny 1999; Man et al. 2001) of salivary glands. The expression of the stem and progenitor cell marker Prominin-1 in those segments of the duct system might be highly relevant in the context of self-renewal and regeneration of these organs. Whether detection of Prominin-1 expression in a particular organ system per se is sufficient for scoring for the presence of either somatic stem cells or cells exhibiting a capacity of de-differentiation (Florek et al. 2005), needs further careful evaluation. Nevertheless, direct prospective isolation of Prominin-1 populations might open up in the future new avenues for assessing the potential of phenotypic switch (trans-differentiation) capabilities of these cell populations.

The analysis of the meibomian gland, the big sebaceous gland of the *tarsus*, also yielded interesting details as to the differential expression of the two Prominin paralogues. In this gland, Prominin-1 was barely detectable as opposed to the expression of Prominin-2. As a side finding, we have revealed that the eyelash, one of the ectodermal appendages located in the vicinity of the meibomian gland, is also positive for Prominin-2, but not for Prominin-1. In this context, the expression of Prominin-2 seems to be associated with modified hair structures being highly sensitive for tactile stimuli. In agreement with this notion, Prominin-2 is detected in the invaginating epithelium of the developing whiskers (*vibrissae*) of fetal mice (J. Jászai and D. Corbeil, unpublished data) as well. In contrast, Prominin-1 seems to be rather associated with mesenchymal cells than epithelial ones, since this molecule is detectable only in the dermal papilla cells of the developing and regenerating murine hair and not in the root-sheath (Ito et al. 2007).

Interestingly both Prominin paralogues can be detected in the saliva where they are associated with small membrane particles that are sedimented upon high-speed centrifugation as those previously reported in the urine (Marzesco et al. 2005; Florek et al. 2007). The amount of Prominin-2 in saliva seems to be significantly lower than those of Prominin-1, which might partly reflect the succinct differences existing in their subcellular compartmentalization. Prominin-1 being restricted to microvilli and cilia present at the apical (luminal) membrane domain (Weigmann et al. 1997; Dubreuil et al. 2007; Florek et al. 2007), whereas Prominin-2 is mainly located in plasma membrane protrusions found in the basolateral domain of polarized epithelial cells (Florek et al. 2007; J. Jászai and D. Corbeil, unpublished data). It remains elusive if the Prominin-1-and/or Prominin-2-containing membrane particles could carry any morphogenetic information as was shown for Sonic hedgehog and retinoic acid containing ‘vesicular parcels’ in the murine node (Tanaka et al. 2005). Although, the physiological relevance of the Prominin-containing membrane particles in the saliva is not yet clear, their easy accessibility might be valuable for diagnostic purposes. An inherited form of progressive retinal degeneration is particularly relevant in this context (Maw et al. 2000; Jászai et al. 2007). A point mutation in the human *PROMININ-1* gene results in the translation of a truncated protein product in the affected individuals (Maw et al. 2000). This mutant form of Prominin-1 is not transported to the cell surface, but instead degraded in the endoplasmic reticulum, hence potentially decreasing the Prominin-1 content of the saliva. Beyond inherited disorders, various excretory organs, e.g., salivary glands, kidney, affected by solid tumors might also be particularly interesting objects of “prominin detection-based” diagnostic efforts. Recently, we have demonstrated an up-regulation of Prominin-1 expression in various renal- and

prostate-tumors in zones surrounding the malignantly transformed regions (Florek et al. 2005; Missol-Kolka et al. manuscript in preparation) holding a potential for increased excretion of this molecule into the corresponding body fluids. Whether elevated expression would also be detected in various salivary gland neoplasias is not documented yet, but it will be interesting to evaluate. Finally, analyzing the prominin content, in conjunction with other constituents of the saliva, might also be an important tool for monitoring functional recovery of salivary glands after progenitor cell transplantation.

Acknowledgments We thank Suzanne Manthey and Ina Lehmann for the skillful assistance for preparing the cryosection samples. W. B. H. was supported by the Deutsche Forschungsgemeinschaft (SPP 1109, Hu275/7-3; SPP 1111, Hu275/8-3; SFB/TR13-04 B1; SFB 655 A2) and D. C. by the Deutsche Forschungsgemeinschaft (SPP 1109, CO 298/2-2; SFB/TR13-04 B1; SFB 655 A13) and Sächsisches Ministerium für Wissenschaft und Kunst-Europäischer Fond für Regionale Entwicklung (4212/05-16).

References

- Corbeil D, Röper K, Hellwig A, Taviam M, Miraglia S, Watt SM, Simmons PJ, Peault B, Buck DW, Huttner WB (2000) The human AC133 hematopoietic stem cell antigen is also expressed in epithelial cells and targeted to plasma membrane protrusions. *J Biol Chem* 275:5512–5520
- Corbeil D, Röper K, Fargeas CA, Joester A, Huttner WB (2001a) Prominin: a story of cholesterol, plasma membrane protrusions and human pathology. *Traffic* 2:82–91
- Corbeil D, Fargeas CA, Huttner WB (2001b) Rat prominin, like its mouse and human orthologues, is a pentaspan membrane glycoprotein. *Biochem Biophys Res Commun* 4:939–944
- Cutler LS, Chaudhry AP (1974) Cytodifferentiation of the acinar cells of the rat submandibular gland. *Dev Biol* 41:31–41
- Cutler LS, Chaudhry AP (1975) Cytodifferentiation of striated duct cells and secretory cells of the convoluted granular tubules of the rat submandibular gland. *Am J Anat* 143:201–217
- Cutler LS, Gremski W (1991) Epithelial-mesenchymal interactions in the development of salivary glands. *Crit Rev Oral Biol Med* 2:1–12
- Denny PC, Ball WD, Redman RS (1997) Salivary glands: a paradigm for diversity of gland development. *Crit Rev Oral Biol Med* 8:51–75
- Denny PC, Denny PA (1999) Dynamics of parenchymal cell division, differentiation, and apoptosis in the young adult female mouse submandibular gland. *Anat Rec* 254:408–417
- Dubreuil V, Marzesco AM, Corbeil D, Huttner WB, Wilsch-Bräuninger M (2007) Midbody and primary cilium of neural progenitors release extracellular membrane particles enriched in the stem cell marker prominin-1. *J Cell Biol* 176:483–495
- Entesarian M, Matsson H, Klar J, Bergendal B, Olson L, Arakaki R, Hayashi Y, Ohuchi H, Falahat B, Bolstad AI, Jonsson R, Wahren-Herlenius M, Dahl N (2005) Mutations in the gene encoding fibroblast growth factor 10 are associated with aplasia of lacrimal and salivary glands. *Nat Genet* 37:125–127
- Fargeas CA, Florek M, Huttner WB, Corbeil D (2003a) Characterization of prominin-2, a new member of the prominin family of pentaspan membrane glycoproteins. *J Biol Chem* 278:8586–8596
- Fargeas CA, Corbeil D, Huttner WB (2003b) AC133 antigen, CD133, prominin-1, prominin-2, etc.: prominin family gene products in need of a rational nomenclature. *Stem Cells* 21:506–508
- Fargeas CA, Fonseca A-V, Huttner WB, Corbeil D (2006) Prominin-1 (CD133)—from progenitor cells to human diseases. *Future Lipidol* 1:213–225
- Florek M, Haase M, Marzesco AM, Freund D, Ehninger G, Huttner WB, Corbeil D (2005) Prominin-1/CD133, a neural and hematopoietic stem cell marker, is expressed in adult human differentiated cells and certain types of kidney cancer. *Cell Tissue Res* 319:15–26
- Florek M, Bauer N, Janich P, Wilsch-Bräuninger M, Fargeas CA, Marzesco AM, Ehninger G, Thiele C, Huttner WB, Corbeil D (2007) Prominin-2 is a cholesterol-binding protein associated with apical and basolateral plasmalemmal protrusions in polarized epithelial cells and released into urine. *Cell Tissue Res* 328:31–47
- Gresik EW, MacRae EK (1975) The postnatal development of the sexually dimorphic duct system and of amylase activity in the submandibular glands of mice. *Cell Tissue Res* 157:411–422
- Gresik EW (1994) The granular convoluted tubule (GCT) cell of rodent submandibular glands. *Microsc Res Tech* 27:1–24
- Gresik EW, Hosoi K, Kurihara K, Maruyama S, Ueha T (1996) The rodent granular convoluted tubule cell—an update. *Eur J Morphol* 34:221–224
- Hand AR, Sivakumar S, Barta I, Ball WD, Mirels L (1996) Immunocytochemical studies of cell differentiation during rat salivary gland development. *Eur J Morphol* 34:149–154
- Hebel R, Stromberg MW (1976) Anatomy of the laboratory rat. The Williams & Wilkins Company, Baltimore, MD, USA, pp 44–46
- Ito Y, Hamazaki TS, Ohnuma K, Tamaki K, Asashima M, Okochi H (2007) Isolation of murine hair-inducing cells using the cell surface marker prominin-1/CD133. *J Invest Dermatol* 127:1052–1060
- Jászai J, Fargeas CA, Florek M, Huttner WB, Corbeil D (2007) Focus on molecules: prominin-1 (CD133). *Exp Eye Res* [Epub ahead of print; doi:10.1016/j.exer.2006.03.022]
- Kagami H, Hiramatsu Y, Hishida S, Okazaki Y, Horie K, Oda Y, Ueda M (2000) Salivary growth factors in health and disease. *Adv Dent Res* 14:99–102
- Lardon J, Corbeil D, Huttner WB, Ling Z, Bouwens L (2007) Stem cell marker prominin 1/AC133 is expressed in duct cells of the adult human pancreas. *Pancreas* (in press)
- Man YG, Ball WD, Culp DJ, Hand AR, Moreira JE (1995) Persistence of a perinatal cellular phenotype in submandibular glands of adult rat. *J Histochem Cytochem* 43:1203–1215
- Man YG, Ball WD, Marchetti L, Hand AR (2001) Contributions of intercalated duct cells to the normal parenchyma of submandibular glands of adult rats. *Anat Rec* 263:202–114
- Marzesco A-M, Janich P, Wilsch-Bräuninger M, Dubreuil V, Langenfeld K, Corbeil D, Huttner WB (2005) Release of extracellular membrane particles carrying the stem cell marker prominin-1 (CD133) from neural progenitors and other epithelial cells. *J Cell Sci* 118:2849–2858
- Maw MA, Corbeil D, Koch J, Hellwig A, Wilson-Wheeler JC, Bridges RJ, Kumaramanickavel G, John S, Nancarrow D, Röper K, Weigmann A, Huttner WB, Denton MJ (2000) A frameshift mutation in prominin (mouse)-like 1 causes human retinal degeneration. *Hum Mol Genet* 9:27–34
- McCulley JP, Shine WE (2004) The lipid layer of tears: dependent on meibomian gland function. *Exp Eye Res* 78:361–365
- Miraglia S, Godfrey W, Yin AH, Atkins K, Warnke R, Holden JT, Bray RA, Waller EK, Buck DW (1997) A novel five-transmembrane hematopoietic stem cell antigen: isolation, characterization, and molecular cloning. *Blood* 90:5013–5021
- Okumura K, Nakamura K, Hisatomi Y, Nagano K, Tanaka Y, Terada K, Sugiyama T, Umeyama K, Matsumoto K, Yamamoto T, Endo F (2003) Salivary gland progenitor cells induced by duct ligation differentiate into hepatic and pancreatic lineages. *Hepatology* 38:104–113

- Patel VN, Rebutini IT, Hoffman MP (2006) Salivary gland branching morphogenesis. *Differentiation* 74:349–364
- Redman RS, Ball WD (1978) Cytodifferentiation of secretory cells in the sublingual gland of the prenatal rat: a histological, histochemical and ultrastructural study. *Am J Anat* 153:367–389
- Shimazaki J, Goto E, Ono M, Shimmura S, Tsubota K (1998) Meibomian gland dysfunction in patients with Sjogren syndrome. *Ophthalmology* 105:1485–1488
- Takahashi S, Schoch E, Walker NI (1998) Origin of acinar cell regeneration after atrophy of the rat parotid induced by duct obstruction. *Int J Exp Pathol* 79:293–301
- Tanaka Y, Okada Y, Hirokawa N (2005) FGF-induced vesicular release of Sonic hedgehog and retinoic acid in leftward nodal flow is critical for left-right determination. *Nature* 435:172–177
- Tandler B (1993) Structure of the duct system in mammalian major salivary glands. *Microsc Res Tech* 26:57–74
- Tandler B, Gresik EW, Nagato T, Phillips CJ (2001) Secretion by striated ducts of mammalian major salivary glands: review from an ultrastructural, functional, and evolutionary perspective. *Anat Rec* 264:121–145
- Tiveron MC, Hirsch MR, Brunet JF (1996) The expression pattern of the transcription factor Phox2 delineates synaptic pathways of the autonomic nervous system. *J Neurosci* 16:7649–7660
- Tran SD, Wang J, Bandyopadhyay BC, Redman RS, Dutra A, Pak E, Swaim WD, Gerstenhaber JA, Bryant JM, Zheng C, Goldsmith CM, Kok MR, Wellner RB, Baum BJ (2005) Primary culture of polarized human salivary epithelial cells for use in developing an artificial salivary gland. *Tissue Eng* 11:172–181
- Yin AH, Miraglia S, Zanjani ED, Almeida-Porada G, Ogawa M, Leary AG, Olweus J, Kearney J, Buck DW (1997) AC133, a novel marker for human hematopoietic stem and progenitor cells. *Blood* 90:5002–5012
- van Blokland SC, Versnel MA (2002) Pathogenesis of Sjogren's syndrome: characteristics of different mouse models for autoimmune exocrinopathy. *Clin Immunol* 103:111–124
- Weigmann A, Corbeil D, Hellwig A, Huttner WB (1997) Prominin, a novel microvilli-specific polytopic membrane protein of the apical surface of epithelial cells, is targeted to plasmalemmal protrusions of non-epithelial cells. *Proc Natl Acad Sci USA* 94:12425–12430
- Wolff MS, Mirels L, Lagner J, Hand AR (2002) Development of the rat sublingual gland: a light and electron microscopic immunocytochemical study. *Anat Rec* 266:30–42
- Zajicek G, Yagil C, Michaeli Y (1985) The streaming submandibular gland. *Anat Rec* 213:150–158
- Zelles T, Purushotham KR, Macauley SP, Oxford GE, Humphreys-Beher MG (1995) Saliva and growth factors: the fountain of youth resides in us all. *J Dent Res* 74:1826–1832
- Zhang Q, Haleem R, Cai X, Wang Z (2002) Identification and characterization of a novel testosterone-regulated prominin-like gene in the rat ventral prostate. *Endocrinology* 143:4788–4796